Mathematical and Computational Applications

MDPI

Article

IoTToe: Monitoring Foot Angle Variability for Health Management and Safety †

Ata Jahangir Moshayedi [1], Zeashan Khan [2,*], Zhonghua Wang [1] and Mehran Emadi Andani [3]

[1] School of Information Engineering, Jiangxi University of Science and Technology, Ganzhou 341000, China; ajm@jxust.edu.cn (A.J.M.); wangzhua131@gmail.com (Z.W.)
[2] Interdisciplinary Research Center for Intelligent Manufacturing and Robotics (IRC-IMR), King Fahd University of Petroleum and Minerals (KFUPM), Dhahran 31261, Saudi Arabia
[3] Department of Neurosciences, Biomedicine and Movement Sciences, University of Verona, 37129 Verona, Italy; mehran.emadiandani@univr.it
* Correspondence: zeashan.khan@kfupm.edu.sa
† This is a revised and extended version of the paper published in Moshayedi, A.J.; Iskar, I.; Yang, S.; Shinde, S.K.; Razi, A.; Andani, M.E. IOTToe: A Smart System for In/Out-Toeing Foot Identification. In Proceedings of the 2024 6th International Conference on Communications, Information System and Computer Engineering (CISCE), Guangzhou, China, 10–12 May 2024; IEEE: Piscataway, NJ, USA, 2024.

Abstract

Toe-in (inward) and toe-out (outward) foot alignments significantly affect gait, posture, and joint stress, causing issues like abnormal gait, joint strain, and foot conditions such as plantar fasciitis and high arches. Addressing these alignments is crucial for improving mobility and comfort. This study introduces IoTToe, a wearable IoT device designed to detect and monitor gait patterns by using six ADXL345 sensors positioned on the foot, allowing healthcare providers to remotely monitor alignment via a webpage, reducing the need for physical tests. Tested on 45 participants aged 20–25 years with diverse BMIs, IoTToe proved suitable for both children and adults, supporting therapy and diagnostics. Statistical tests, including ICC, DFA, and ANOVA, confirmed the device's effectiveness in detecting gait and postural control differences between legs. Gait variability results indicated that left leg showed more adaptability (DFA close to 0.5), compared to the right leg which was found more consistent (DFA close to 1). Postural control showed stable and agile standing with values between 0.5 and 1. Sensor combinations revealed that removing sensor B (on the gastrocnemius muscle) did not affect data quality. Moreover, taller individuals displayed smaller ankle angle changes, highlighting challenges in balance and upper body stability. IoTToe offers accurate data collection, reliability, portability, and significant potential for gait monitoring and injury prevention. Future studies would expand participation, especially among women and those with alignment issues, to enhance the system's applicability for foot health management, safety and rehabilitation, further supporting telemetric applications in healthcare.

Keywords: in-toeing feet; out-toeing feet; Achilles tendon; instep; Internet of Things (IoT); injury prevention

Check for updates

Received: 5 November 2025
Revised: 26 December 2025
Accepted: 10 January 2026
Published: 16 January 2026

Copyright: © 2026 by the authors. Licensee MDPI, Basel, Switzerland. This article is an open access article distributed under the terms and conditions of the Creative Commons Attribution (CC BY) license.

1. Introduction

The weight of the human body is borne by the feet; therefore, foot alignment is a critical factor in overall biomechanical health. Proper foot alignment ensures biomechanical efficiency, reduces muscle strain and injury risk, supports correct posture, and helps alleviate pain [1]. As illustrated in Figure 1, the concept of foot alignment plays a key role

in evenly distributing forces across the foot, thereby helping to prevent common overuse injuries such as plantar fasciitis and shin splints [2]. Correct foot mechanics enhance balance and stability, crucial for older adults, and improve athletic performance by boosting speed, agility, and endurance [3]. Additionally, maintaining good foot form promotes long-term joint health and overall comfort during physical activities, encouraging a more active lifestyle (Figure 1A).

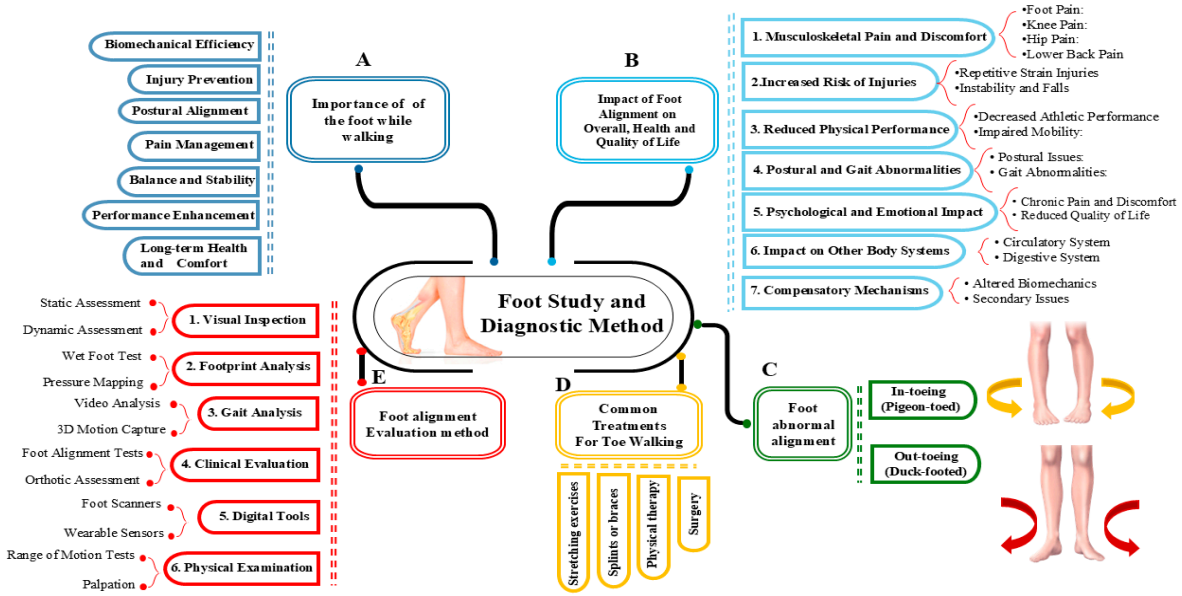


Figure 1. Analysis of Foot Alignment and Related Issues. (**A**) Importance of foot alignment in walking; (**B**) Foot alignment and its side effects; (**C**) Two main foot abnormalities; (**D**) Common treatments for toe walking; (**E**) Methods for evaluating foot alignment.

Poor foot alignment (Figure 1B) can lead to musculoskeletal pain in the feet, knees, hips, and lower back, increasing the risk of injuries and reducing physical performance. It can cause gait and postural abnormalities, impacting mobility and quality of life [4]. Additionally, chronic pain resulting from foot misalignment can negatively affect mental health and overall quality of life, while compensatory movement strategies may lead to secondary musculoskeletal disorders [5]. Among the most common forms of improper foot alignment are in-toeing and out-toeing gait patterns [6], as illustrated in Figure 1C where the former is characterized by the feet pointing inward rather than straight ahead and is often associated with structural abnormalities such as metatarsus adductus or femoral anteversion, as well as neuromuscular conditions including cerebral palsy [7]. The later anomaly is typically caused by conditions like external tibial torsion or femoral retroversion which can result from genetic predisposition and are commonly seen in young children [8]. While they may ameliorate with growth, persistent cases might require medical intervention. Treatment options range from physiotherapy to orthopedic braces or surgery [9].

Early diagnosis and appropriate management are essential to prevent long-term complications and to promote normal gait development. Regular clinical follow-ups play a critical role in monitoring progression and evaluating treatment effectiveness [10]. Gait abnormalities vary in prevalence and severity, with most mild cases resolving spontaneously; however, more severe manifestations can significantly impair mobility and necessitate medical intervention, as shown in Figure 1D. One particularly challenging condition is persistent or idiopathic causes, which may require prolonged treatment and continuous monitoring. Progress is often gradual, and therapeutic interventions while effective can demand substantial time and resources, with improvements not always immediately apparent [11]. Consequently, sustained

engagement from parents and caregivers, along with consistent follow-up appointments, is crucial. If toe walking does not improve under current treatment protocols, further clinical evaluation or alternative interventions may be required [12]. Designing and developing a system that can observe, detect issues and report on improvements via an IoT-based sensing platform could benefit this treatment process, which serves as the main target of this research. Our novel contributions are listed as follows:

1. Implement multi-point data acquisition using Inertial Measurement Units (IMUs) to comprehensively monitor the foot rotation and linear movement, thereby enriching the data for subsequent analysis.
2. Design a portable and user-friendly device with a simple structure for easy wearability and biomechanical analysis empowered with IoT capabilities to enable remote monitoring without the need for a doctor's presence during testing. The device can accurately capture foot movement from multiple angles and positions.
3. Develop data visualization with line charts to facilitate intuitive understanding of gait data for both professionals and users.
4. Enable practical clinical application by providing accurate foot rotation data for developing personalized treatment plans and rehabilitation strategies.

The authors believe that this design holds significant importance for a wide range of individuals. For those experiencing pronation issues, the system provides timely monitoring and feedback, raising awareness and guiding appropriate rehabilitation to prevent further injuries and discomfort. Additionally, for professionals who spend long hours standing or walking, such as service workers or construction personnel, this project acts as a health companion, helping to prevent pain and fatigue caused by abnormal gait, thereby enhancing work efficiency and quality of life.

The paper is organized as follows: Section 2 outlines the related work. Section 3 details the design structure, including hardware while Section 4 details software descriptions, data preparation, and analysis including, test statistics and protocols, environment, metrics, and results. Finally, Section 5 provides the conclusion. This paper extends our previous conference paper, "IoTToe: A Smart System for In/Out-Toeing Foot Identification," which was accepted and presented at the IEEE 6th International Conference on Communications, Information System and Computer Engineering (CISCE 2024) [13].

2. Related Work

A review of published research papers on the design and development of foot alignment systems is conducted to document previous works. For example, Mancinelli et al. (2009) explored the use of a sensor integrated footwear to monitor gait abnormalities in children with cerebral palsy, focusing on the equinus (toe-walking) gait pattern. By analyzing features from center of pressure trajectories and ankle kinematics, the study proved that a classifier can predict the severity of toe-walking with high accuracy. It is suggested that the sensorized shoe could be a valuable tool for frequent, objective gait assessments, potentially improving clinical management [14]. Senanayake et al. (2010) presented an intelligent gait-phase detection algorithm that leverages fuzzy logic to handle the complexities of varying gait parameters, using real-time data from force-sensitive resistors and inertial sensors. The system effectively detected gait phases, used to identify abnormalities and provide accurate feedback timing. A software application was also developed to manage the extensive data required for quality gait analysis. The study identified that most errors occurred during the stance phase, primarily due to varying shoe sizes among subjects, suggesting the need for customized insoles to improve accuracy. Comparative analysis showed the proposed system performed better than several existing methods, though

further enhancement using advanced machine learning techniques could improve accuracy despite potential increases in computational complexity [15].

Schoepflin et al. (2010) developed a novel bio-driven mobile-assistive device for toddlers, controlled by foot motion to enhance gross motor skill development while providing independent mobility. The feasibility was tested on five normal toddlers and one with spastic Cerebral Palsy (CP). All were able to successfully navigate a maze using the device. The study suggested that the device is intuitive, supports motor development, and offers potential for real-world applications. Future improvements could include reducing the device's size, enhancing camera accuracy, and further refining the control interface for children with mobility impairments [16]. The study by Mancinelli et al. (2012) introduced Active Gait, a novel sensorized shoe system designed to monitor and classify the severity of gait deviations in children with CP by addressing the limitations of current clinical practices, which rely on infrequent assessments in controlled environments using home-based evaluations. Active Gait captures data on gait deviations through Center of Pressure (CoP) trajectories and employs a Random Forest classifier to estimate severity scores based on the Edinburgh Visual Scale. Preliminary testing involved 11 children with varying degrees of CP-related gait deviations. The results demonstrated that the classifier achieved over 80% accuracy for six out of seven observations in field testing, indicating the system's feasibility for clinical use. Additionally, the system showed over 90% accuracy in home-based testing for a single subject, suggesting that gait assessments in natural environments may provide a more accurate reflection of a child's condition compared to controlled settings concluding that Active Gait has the potential to become a valuable tool for longitudinal monitoring of gait severity in children with CP [17]. Farago et al. (2020) introduced a wearable system to assess gait biomechanics by cross-correlating plantar pressure from insole sensors with EMG data from lower-limb muscles. The system generates a gait map to distinguish normal from pathological walking. Validated in a lab, it showed great potential for clinical applications in detecting gait abnormalities and muscle dysfunction. Future work aims to miniaturize the device for broader use in rehabilitation and gait analysis [18].

Zhang et al. (2022) developed a method for real-time gait phase estimation in multi-locomotion modes using Inertial Measurement Units (IMUs). They employed a Long Short-Term Memory (LSTM) network for gait pattern recognition and a Dual Adaptive Frequency Oscillator (DAFO) for continuous phase estimation. The approach achieved a 98.58% classification accuracy with an F1 score of 0.9875 and effectively detected toe-off events with an average error of 15.34 ± 40.58 ms. The method shows improved stability over traditional models and suggests future work on reducing IMU count, predicting gait phases, expanding datasets, and including additional gait events [19].

Xia et al. (2020) introduced a haptic feedback-sensorized shoe designed for modifying foot progression angle (FPA) during walking. The shoe features an inertial and magnetometer module for FPA estimation and vibration motors for providing feedback. Feasibility tests showed an overall FPA performance error of $0.2 \pm 4.1^{\circ}$, with a mean absolute error of $3.1 \pm 2.6^{\circ}$. Reducing the no-feedback window improved performance. This shoe offers a portable, non-laboratory-based solution for FPA modification, potentially benefiting knee osteoarthritis treatment and other clinical applications [20].

Mani et al. (2020) developed a wearable ultrasonic-based system for gait analysis that directly measures ankle angle (AA) and toe clearance (MTC) without complex sensor fusion algorithms. This system uses triangulation methods to avoid issues with drift in inertial measurement units (IMUs). Tested against a video-based reference, the system showed root mean square errors of 0.91 to 1.54 degrees for AA and 0.36 to 1.26 cm for MTC. The repeatability ranged from 1.53 to 2.56 degrees for AA and 0.27 to 1.42 cm for MTC. The system demonstrated strong correlations ($r = 0.98$ for AA and $r = 0.99$ for MTC) with

normative gait patterns, suggesting its efficacy for continuous gait monitoring [21]. Wu et al. (2021) developed an intelligent in-shoe system for real-time gait monitoring, focusing on optimized sampling frequency to ensure high signal fidelity. Their system addresses the limitations of previous wearable sensors by enhancing data acquisition bandwidth. In validation with an optical motion capture system across 20 sessions with four subjects, the system achieved percentage mean absolute errors of 1.19% for stride time, 1.68% for stride length, 2.08% for stride velocity, and 1.23% for cadence. Additionally, they introduced a new gait metric using eigen analysis and principal component analysis to differentiate gait patterns, showing promise for gait disorder diagnostics [22].

Martínez-Barba et al. (2020) introduced a self-calibrating sensor-footwear system designed for plantar pressure distribution (PPD) measurements. The system adjusts the force measurement range (FMR) to user weight, with options ranging from 0 to 25 N to 0–200 N, enhancing force resolution. The study highlights that sensor responses vary across different footwear sections (back, middle, front), and a coefficient of variation (CV) of 2.62% was observed before installation, increasing to 16.61% after installation. To address this, the authors developed an in-shoe characterization method to standardize sensor responses and ensure accurate force readings. The footwear system, equipped with wireless communication for real-time PPD visualization and recording, demonstrates the critical role of in-shoe sensor calibration [23].

Wouda et al. (2021) developed a method to estimate the foot progression angle (FPA) using a single foot-worn inertial sensor (accelerometer and gyroscope). Their approach involves recalculating a dynamic step frame during each step's stance phase to minimize drift and avoid using a magnetometer. The FPA is determined as the angle between the walking direction and this dynamic frame. Validated with five subjects across three gait types (normal, toe-in, toe-out), the method achieved a maximum mean error of 2.6° and effectively distinguished between gait types. This approach offers a practical solution for FPA estimation in various environments, including those with magnetic distortions [24]. Xu et al. (2021) designed a low-cost gait-recognition system for children to classify pathological gaits using an 8×8 pressure-sensor array. Their method, known as the intelligent gait-recognition method (IGRM), relies on machine learning to analyze plantar pressure data in both static and dynamic settings. The system was tested with 17 children to recognize three pathological gaits (toe-in, toe-out, and flat) and normal gait. The IGRM achieved 92.41% and 97.79% intra-subject recognition accuracy, and 85.78% and 78.81% inter-subject recognition accuracy in static and dynamic conditions, respectively. The system demonstrated high precision and real-time performance, making it a promising tool for monitoring and providing feedback on gait abnormalities in children [25].

Caderby et al. (2022) evaluated two methods for estimating the foot progression angle (FPA) using force-plate data, comparing them to a motion capture system. Ten healthy adults walked at slow, preferred, and fast speeds while FPA was measured. The study found that a novel force-plate method was more accurate and precise than a previously reported method. The novel method had a mean absolute error of $3.3 \pm 2.1°$ at slow speed, and $2.0 \pm 1.2°$ at both preferred and fast speeds, showing no significant speed effect ($p > 0.05$). This novel method provides a valid alternative for measuring FPA in the absence of kinematic data [26]. In another study, Ershadi et al. (2021) introduced the Smart Insole platform, designed for remote monitoring and feedback of toe walking patterns, which involves walking on the toes without heel contact, leading to serious foot and muscle issues. The Smart Insole uses two pressure sensors to detect walking patterns and triggers vibrations to alert users when toe walking is detected. The algorithm achieved an average accuracy of 91.3% in distinguishing between toe walking, heel-to-toe walking, sitting, and

standing. This platform aids in gait rehabilitation by providing accurate monitoring and feedback, supporting orthopedic professionals in managing toe walking [27].

Prasanth et al. (2021) reviewed wearable sensors for real-time gait analysis, highlighting the shift from costly lab-based systems to more accessible, affordable options. They found IMUs and insole pressure sensors most common, with rule-based methods like threshold detection frequently used. Heel strike and toe-off events were noted as key focus areas. The review recommends combining IMUs with rule-based techniques for effective gait detection and emphasizes the need for validation on target populations. Future research should standardize performance metrics and consider clinical applications to enhance rehabilitation for gait impairments [28]. Ardhianto et al. (2022) developed a deep learning model based on YOLO (You Only Look Once) for detecting foot progression angle (FPA) using plantar pressure images to address gait pathologies. They tested three YOLO networks (v3, v4, v5x) on 1424 images, finding YOLOv4 to have the highest accuracy. YOLOv4 achieved an average precision of 100% for left foot and 99.78% for right foot, with FPA measurements closely matching ground-truth values ($5.58 \pm 0.10^{\circ}$). YOLOv3 and YOLOv5x showed less accuracy. The study concludes that YOLOv4 is effective for precise FPA detection, aiding in the assessment of physical therapy impacts on knee conditions [29]. Kim et al. (2022) developed a deep-learning LSTM model for automatically detecting gait events (initial contact (IC) and toe-off (TO)) in children with cerebral palsy using foot-marker kinematics. They analyzed data from 363 subjects and evaluated different marker combinations. The model detected IC with 89.7% accuracy and an 18.5% false alarm rate, but TO detection was less accurate at 71.6% with a 33.8% false alarm rate. The combination of TOE and HEE markers was effective for IC detection, while TO detection varied by gait subgroup, showing 5–10% performance differences. The study suggests LSTM-based detection can improve accuracy and reduce manual annotation efforts [30].

Lee et al. (2022) developed an IoT-based sensor shoe system to monitor and correct gait abnormalities using pressure sensors, a three-axis accelerometer, and a gyroscope. The system identifies pigeon-toed and splay-footed walking patterns, transferring sensor data via Bluetooth to PC and smartphone apps. Gait abnormalities are visually indicated through color changes in the sensors. The system achieved a 56.25% recognition rate for toe-in gait and 81.25% for toe-out gait. It continuously collects and monitors gait data, helping users manage and correct abnormal walking patterns in real-time [31].

Caderby et al. (2022) compares two force-plate methods for estimating foot progression angle (FPA) with a reference motion capture system. The study finds that a novel method based on center of pressure data is more accurate and precise, with mean absolute errors of 3.3° at slow speed and 2.0° at preferred and fast speeds, showing no significant speed effect. This novel method proves to be a valid and effective alternative for measuring FPA without the need for kinematic data [26]. Cao et al. (2024) analyzed the relationship between foot progression angle (FPA), plantar loading, and gait symmetry in children with in toeing using pedobarographic and spatiotemporal data. They found significant correlations between FPA and pressure, force, and impulse in the forefoot and heel regions, particularly in bilateral cases. The study showed that although children exhibit gait self-adjustment, this mechanism weakens as in toeing severity increases, emphasizing the need for early bilateral assessment [32].

Detecting foot alignment involves assessing foot positioning and gait to identify deviations or abnormalities (Figure 1D). Visual inspection includes static assessment of the foot from different angles while standing, and dynamic assessment via walking or running for abnormal movements [33]. Footprint analysis, through wet foot tests and pressure mapping, helps to assess arch height and pressure distribution. Gait analysis uses video and 3D motion capture to evaluate foot strike patterns and alignment [33]. Clinical

evaluation involves specific tests and orthotic assessment by professionals. Digital tools like foot scanners and wearable sensors offer detailed analysis and real-time tracking of foot movements [34]. Physical examination includes range of motion tests and palpation to detect misalignments. These methods enable accurate detection and analysis of foot alignment issues, which can be addressed with corrective footwear, physical therapy, or orthotic devices [35].

Among these methods, IMU sensors offer real-time, precise data of foot and ankle movements, providing comprehensive analysis of foot biomechanics. They enable continuous monitoring in natural environments and are less intrusive compared to traditional methods. However, they can be expensive, complex to interpret, and require proper calibration. In contrast, traditional methods may lack the precision and real-time capabilities of IMUs but are often less costly and simpler to use [36]. IMU based approach enhances diagnostics and intervention effectiveness for foot alignment issues. To detect toe walking, doctors analyze gait metrics such as heel contact, ankle dorsiflexion, knee extension, cadence, and step length. In addition, muscle strength, joint range of motion, and balance are also evaluated. Gait analysis with Inertial Measurement Units (IMUs) measures parameters like foot strike angle, step length, cadence, stance phase, and swing phase, helping identify abnormalities in walking patterns. These metrics assist in diagnosing and understanding the specifics of toe walking. Stretching exercises, Splints or braces, Physical therapy, and Surgery [37,38]. However, few designs address IoT capabilities, particularly those focusing on affordable, long-term solutions that can track improvements over the course of treatment. Despite these advancements, few designs incorporate IoT capabilities, especially those that provide affordable, long-term solutions for tracking improvements over the course of treatment. Addressing these gaps could lead to more comprehensive and accessible tools for foot alignment analysis and monitoring. To this end, the focus of this research paper is the development of an IoT-based wearable design called IOTToe which is tested on real samples to evaluate its efficiency and performance.

3. Proposed Design

The primary focus of this research is the design and implementation of an IOTToe system, structured as illustrated in Figure 2. The design combines acceleration sensors and processor control boards to enable data acquisition on the hardware side. On the software side, the data is displayed on a custom webpage created using HTML, CSS, and JavaScript, allowing users to easily view and interpret the results [13].

(A) IoT Toe Hardware Components: The hardware design system (Figure 2A) comprises three main sections: the Sensor Unit, the Processor, and the Battery. Each component is detailed as follows: In the **(1) Sensor Part:** The system integrates six ADXL345 accelerometers (developed by Analog Devices (ADI), Wilmington, MA, USA), renowned for their versatility in motion detection. These sensors are economical, compatible, and energy-efficient, making them ideal for tilt sensing, motion detection, and gesture recognition. They use digital interfaces like I2C or SPI to provide critical acceleration data for applications in orientation, activity tracking, and robotics. **(2) Processor:** The hardware section utilizes the NodeMCU (ESP8266) (developed by Espressif Systems, Shanghai, China) as the processor. This versatile Wi-Fi module features an integrated microcontroller, offering affordable and low-power connectivity for IoT applications. It includes a built-in TCP/IP protocol stack, supports multiple interfaces (I2C, UART, SPI), and provides flash memory for storage. Its compact size, powerful microcontroller, and cost-effectiveness make it an ideal choice for both novice and experienced developers. **(3) Battery:** The system is powered by a battery with a 5 V, 2 A output and a capacity of 20,000 mAh (74 Wh). This battery provides up to 3 h of operation on a full charge. **(4) Web Monitoring hardware:** The system includes a

web monitoring component accessible via a PC or mobile phone. Users can observe and interact with the created webpage to view real- time data and system status.

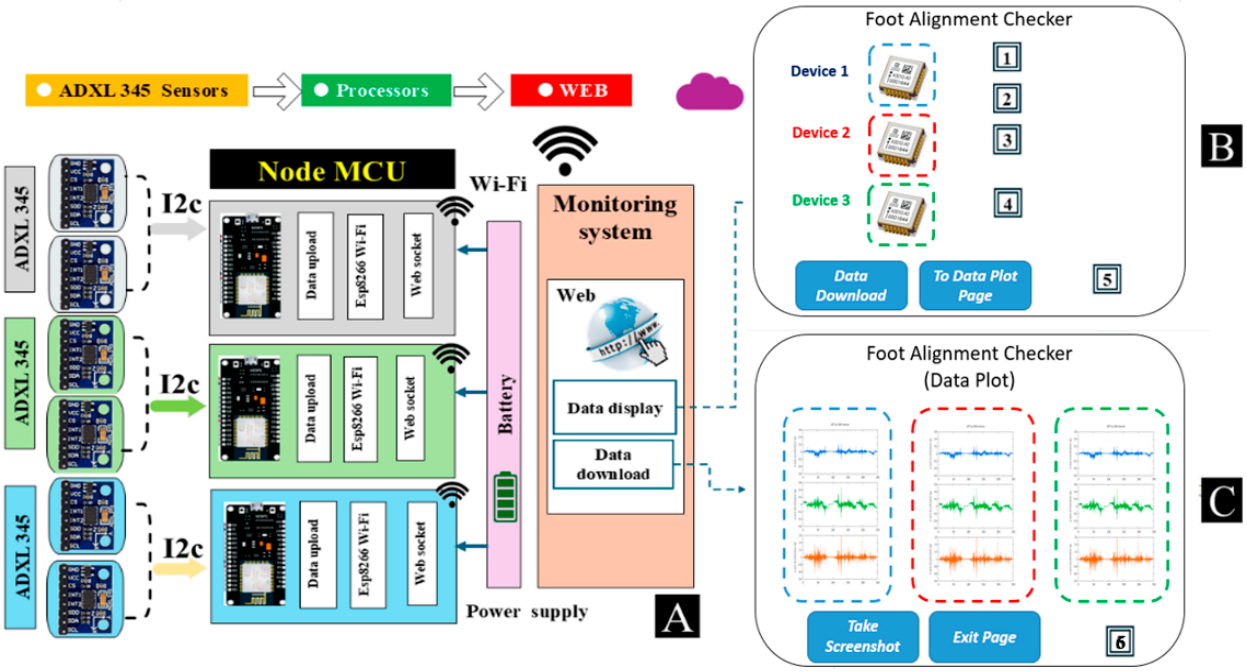


Figure 2. System design and components of IoTToe. (**A**) System includes six AXDL sensors, three NodeMCU modules, a battery, and a web monitoring system. (**B**) Each sensor device (1, 2, and 3) captures data values in the X, Y, and Z directions. (1): the time and date, (2): the X, Y, Z for device one, (3): the X, Y, Z for device two, (4): the X, Y, Z for device three, (5): functional key of data download and switch to plot page. (**C**) The plot page, (6): The graphical representation of sensor data, displayed as charts, provides a clear visualization of the measurements.

(B) Web Monitoring Data: The webpage interface serves three primary functions: displaying sensor values (Figure 2B), offering a download feature, and providing data visualization through a line chart. The NodeMCU transmits processed data to the back-end server, which then processes and displays it on the webpage. This setup enables users to observe real-time data, visualize it through charts, and download it for offline analysis. The section includes the following components: (1) Sensor Data (Figure 2B): This section of the webpage displays real-time charts for six sensors, organized into three devices, with X, Y, and Z readings updated every second. Device 1 comprises Sensor 1 and Sensor 2, Device 2 includes Sensor 3 and Sensor 4, and Device 3 contains Sensor 5 and Sensor 6. (2) Plot Data (Figure 2C): This subsection features a line chart that visualizes sensor data trends, providing a clear view of how data changes over time. (3) Download Section (Figure 2B,C): This section includes a download button that allows users to save real-time data as a local Excel file, improving data accessibility and enabling offline analysis. The front-end of the webpage is developed using a combination of HTML for structure, CSS for styling and layout, and JavaScript for interactivity and dynamic functionality. This approach ensures a responsive and user-friendly interface, enhancing the overall user experience.

(C) IoTToe Software and Algorithm: The three NodeMCU devices collect and transmit data to the server in a predefined format. Each NodeMCU must be connected to a Wi-Fi network, with the server operating on the same local area network (LAN) to ensure continuous data processing. The NodeMCU microcontroller establishes a network connection and communicates with multiple ADXL sensors using SPI or I2C protocols. Once initialized, the NodeMCU connects to the designated Wi-Fi network, enabling remote access. It sets up a web server on the NodeMCU to interact with web clients. The NodeMCU continuously

polls the ADXL sensors, gathering acceleration data in three dimensions: X, Y, and Z axes. This real-time data is temporarily stored in the NodeMCU memory. A web client, such as a browser, connects to the NodeMCU web server through asynchronous requests (AJAX) to request sensor data. Upon receiving these requests, the NodeMCU provides the data to the web client, which dynamically updates an HTML page with interactive plots or visual representations of the acceleration data. The HTML page, enhanced with JavaScript, facilitates dynamic rendering of these plots, allowing users to visualize real-time sensor readings. The NodeMCU continuously streams updated data to the web client, refreshing the plots on the HTML page to ensure users have access to the latest sensor information. This integration of hardware and web technologies enables remote monitoring and visualization of acceleration data, allowing users to gain insights into various physical phenomena or applications in real time. Overall, the proposed design system combines robust hardware with an intuitive software interface, facilitating comprehensive data acquisition, monitoring, and analysis. The use of ADXL345 sensors and ESP8266 modules, alongside a web-based interface, provides a powerful and flexible solution for real-time motion detection and data visualization. Further details about the design and algorithms are provided in [13].

(D) IoT Toe Sensor Location: All six sensors are positioned on both the right and left legs, with three sensor sites considered for each leg. Figure 3 shown in, the setup results in a total of six sensors placed on both feet of the volunteer, with all sensors oriented such that their Z-axis faces upwards, aligning with the foot's direction. As shown in Figure 3, these sites include the instep of the feet, the gastrocnemius muscle, and the Achilles tendon.

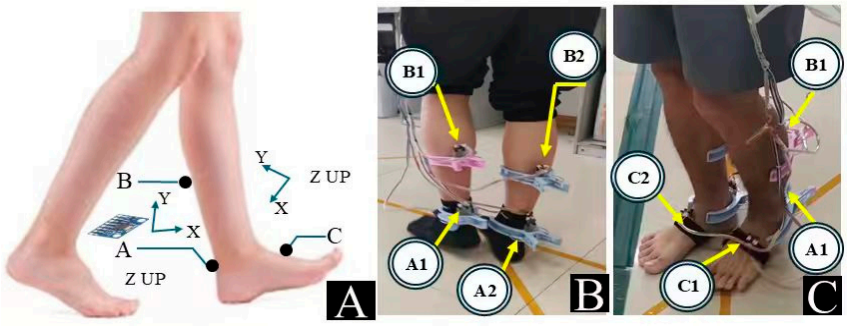


Figure 3. Sensor placement in the IOTToe system. (**A**) Locations of the three sensors on each foot. (**B**) Right-side view of the sensor assembly. (**C**) Front view of the sensor assembly. (A1,A2) Achilles tendon, (B1,B2) Gastrocnemius muscle (calf), (C1,C2) instep of the feet.

The ADXL345 sensors are lightweight, compact, and secured with soft, adjustable straps to minimize pressure and avoid restricting natural foot movement. Cables are carefully routed to prevent obstruction or discomfort. During pilot testing, participants reported no discomfort or limitations in movement, confirming the device's suitability for continuous gait monitoring. From an ergonomic perspective, the low-profile placement and flexible connections allow participants to walk comfortably, ensuring that natural gait patterns are accurately captured.

4. Data Preparation and Analysis

4.1. Data Acquisition

In this project, 45 participants were tested, the sample distribution with respect to Gender (36 male and 9 female). The sample size analysis was calculated a priori using the software G-Power 3.1 (Faul et al., 2007 [39]). Assuming the effect size of 0.25 (which is medium, Cohen, 1988 [40]), the type I error (p-value) of 0.05 to claim statistical significance, the power of 0.95, correlation among repetition of measures of 0.5, and non-sphericity

correction ϵ of 1, the required sample size was 44 (22 for right and left leg). We recorded data from more participants to avoid a potential reduction in power due to dropouts. Forty-five young people (i.e., 90 right and left legs, 7 females, 3 left footed) volunteered for the study (mean ± SD, age: 22.1 ± 1.5 years, body weight: 69.5 ± 21.3 kg, body height: 168.7 ± 7.3 cm, body-mass index: 24.4 ± 7.2 kg/m^2, average steps: 5505 ± 2957 steps/day). All participants received information about the task and the procedure and gave written informed consent prior to the experiment [39,40]. The distribution of sample sizes across genders is due to the limited availability of volunteers for the tests.

As shown in Figure 4, the data provides insights into the demographic characteristics of the participants in terms of age, weight, height, and BMI, highlighting some distinctions between male and female participants in these aspects. Regarding the participant's distribution, with respect to age, the average age for males was approximately 22.28 years, with a range from 20 to 25 years. For female participants, the average age was approximately 21.56 years, with a range from 17 to 24 years. This indicates a slightly younger age profile among female participants. Considering the weight, male participants had an average weight of 63.28 kg approximately, ranging from 160.5 kg to 180 kg while female participants had an average weight of about 55.54 kg, ranging from 144 kg to 175 kg. The data suggests that male participants, on average, had a higher weight compared to female participants. For the height parameter, male participants had an average height of about 171.15 cm, with a range from 45 cm to 86 cm, while female participants had an average height of about 161 cm. This indicates a noticeable difference in height between male and female participants. With respect to body mass index (BMI), the average value for the male participants was approximately 21.58, with a range from 15.57 to 26.56. For female participants, the average BMI was approximately 21.45, with a range from 17.58 to 27.49. To evaluate the reliability and consistency of the measurements across phases, sensor configurations, and gait patterns, we conducted Intraclass Correlation Coefficient (ICC) and Cronbach's alpha analyses that ensure the reproducibility of results while minimizing the effect of random variations [41].

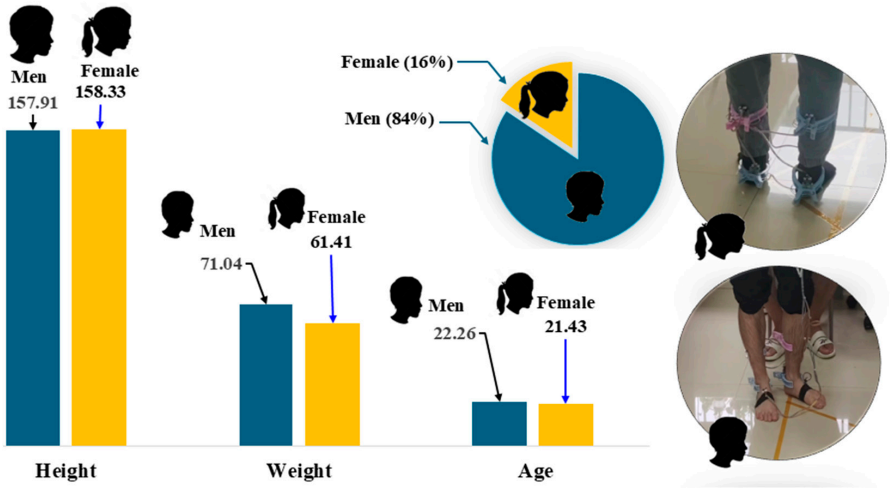


Figure 4. The sample data statics. Pie chart of differences between men and women; bar chart showing the height, weight and age values of participants.

4.2. Test Protocol

The study was conducted in accordance with the ethical standards set forth by the Declaration of Helsinki, and approval was obtained from the Institutional Review Board (IRB) at Jiangxi University of Science and Technology. All participants provided written informed consent before participating in the study. The testing path consists of straight and zigzag routes chosen for evaluating the design data (Figure 5). The test is designed

so that participants must follow a straight path (5.85 m one way, totaling 11.70 m round trip) and a zig zag path (18.85 m round trip), all within a lab room in Jiangxi University of Science and Technology. The zigzag path was selected because it is generally more difficult for individuals with in-toeing or out-toeing. Its sharp direction changes require rapid adjustments in foot placement, which increases joint stress and balance challenges. This makes the zigzag path more demanding compared to a curved path. In contrast, curved paths offer smoother transitions, reducing joint strain and making it easier to maintain consistent foot alignment. By choosing a zigzag path, the focus is on testing the ability to handle these additional challenges [42].

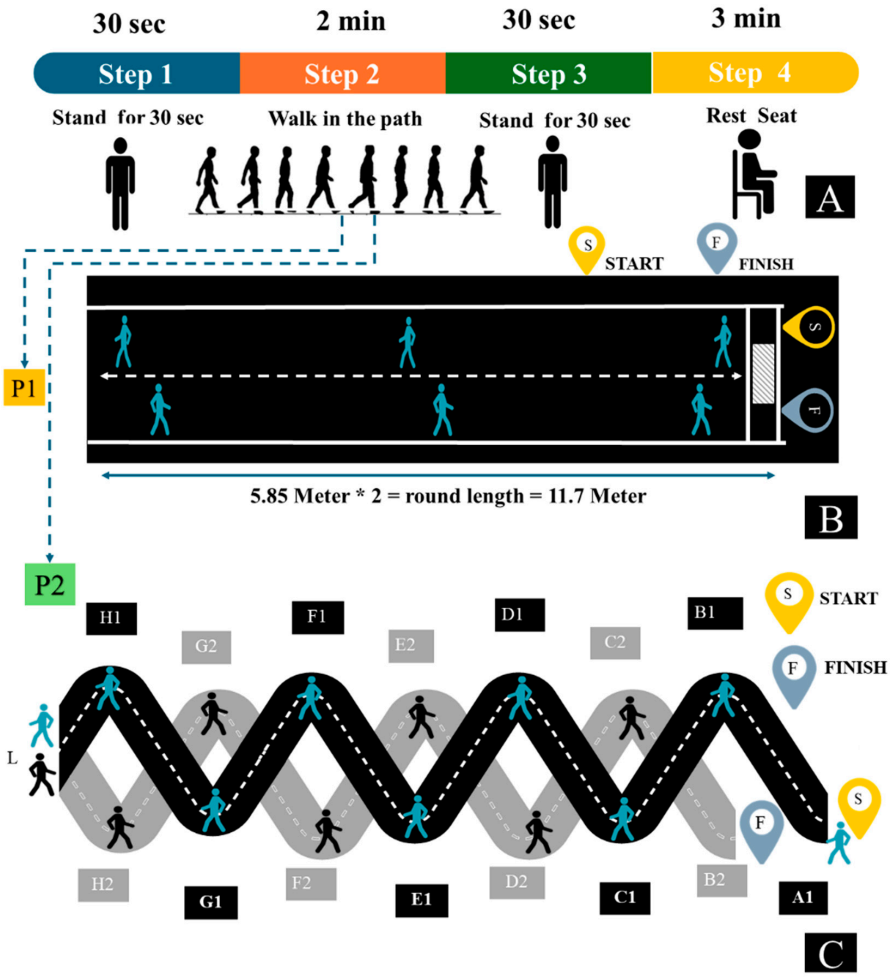


Figure 5. Data collection protocol for straight path (**A**) with each test taking approximately 360 s (5 min), P1: straight path (**B**) total length path of 11.7 m, and P2: Zig Zag path with total length path of 17.495 m (**C**), in the Zigzag path, A1-B1: 124.5 cm, B1-C1: 85.5 cm, C1-D1: 120 cm, D1-E1: 114 cm, E1-F1: 150 cm, F1-G5: 113 cm, G1-H1: 135.5 cm, H1-L: 55 cm, Total: 897.5 cm; L-H2: 64 cm, H2-G2: 154 cm, G2-F2: 130 cm, F2-E2: 122 cm, E2-D2: 147 cm, D2-C2: 113 cm, C2-B2: 122 cm, Total: 852 cm.

The user wears the device to walk along each path, and then follows the path back to the origin point. Before beginning the test, participants are asked to review and sign the "Satisfaction Agreement" (Appendix A.2), which outlines the study's purpose and participation details. They will also be asked to answer qualitative questions in Appendix A.3 which include the demographics, medical and health data, footwear preferences and conditions, as well as walking environment. This information will help to deduce results and support study's objectives after ensuring ethical guidelines of data collection.

The test sequence as mentioned in Figure 5, involved several steps: First, participants stood still for 30 s to record their baseline data. Next, they walked along a predefined path

at a normal speed. After completing the walk, participants waited for 30 s before resting for 3 min while seated. Movement data were recorded in three stages: STG1 (initial 30 s of no movement), STG2 (movement phase), and STG3 (final 30 s of no movement). To ensure data accuracy, each path was tested three times and data was displayed on a web page that is downloadable for analysis. During the walk, the device recorded real-time data, which was then transferred to an Excel file for further analysis. Testing under these varying conditions allowed for a comprehensive evaluation of the device's performance across different scenarios. As mentioned before, data collection for the proposed IoTToe design involved 45 volunteers walking on both straight and zig-zag paths, with data collected for the right and left legs. To obtain accurate data, each path was tested three times as shown in Figure 6.

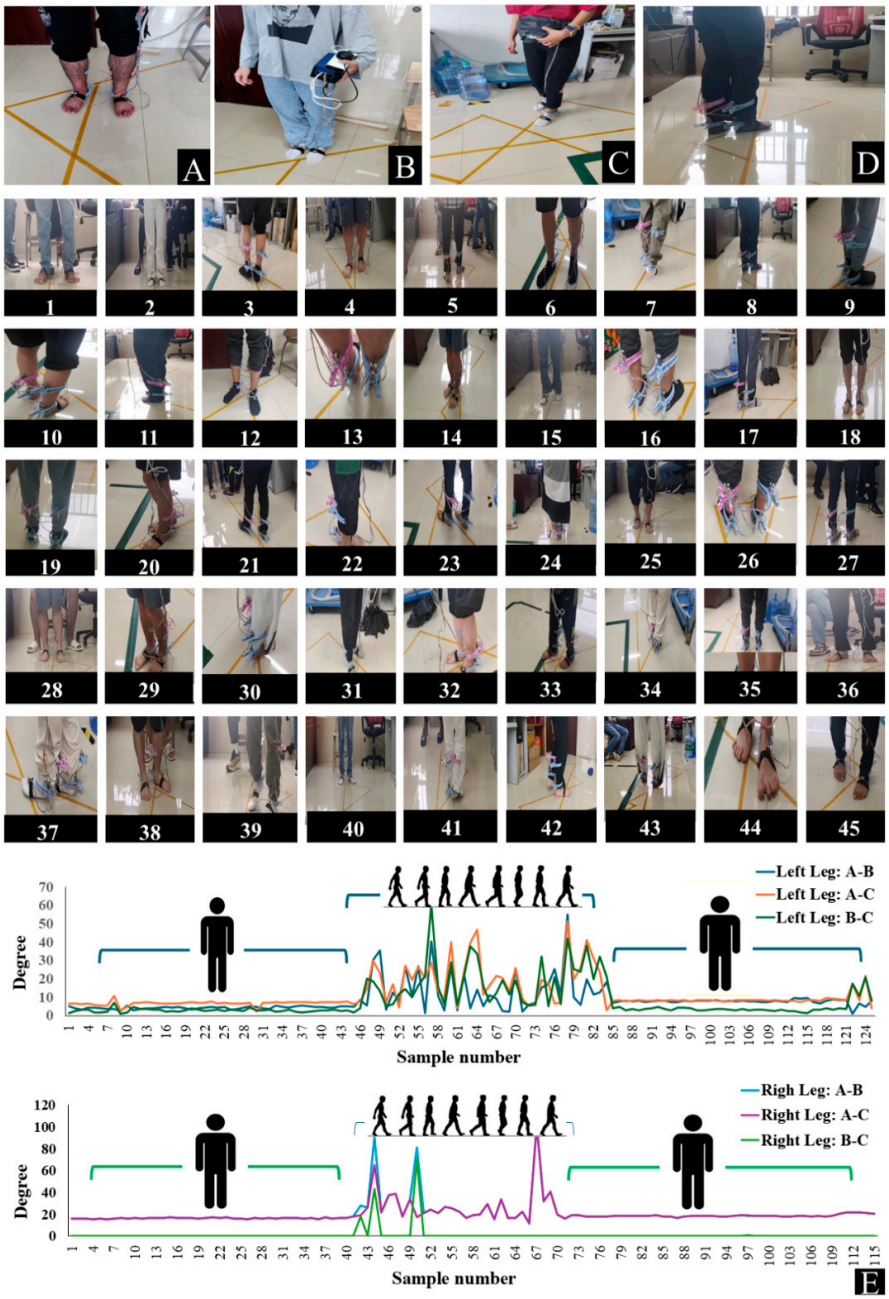


Figure 6. Data collection for the IoTToe design study involved 45 volunteers. (**A**,**C**) Data from the straight walk path, collected separately for the right and left legs. (**B**,**D**) Data from the curved path, with similar leg-specific measurements. (**E**) IoTToe result data based on the proposed sampling protocol for the straight walk path, showing performance for both the right and left legs.

4.3. Metrics

For calculating the sensor data, Equation (1) was used to determine the angle in degrees between two sensors. Considering each sensors X, Y and Z (Sensor A: (X_1, Y_1, Z_1), Sensor B: (X_2, Y_2, Z_2), Sensor C: (X_3, Y_3, Z_3)). The angle between each two sensors can be calculated based on Equation (1).

$$\begin{aligned}\text{Angle sensor A to B} &= cos^{-1}\left(\min\frac{X_1\times X_2+Y_1\times Y_2+Z_1\times Z_2}{\sqrt{\left({X_1}^2+{Y_1}^2+{Z_1}^2\right)\cdot\left({X_2}^2+{Y_2}^2+{Z_2}^2\right)}},1\right)\times\frac{180}{\pi}\\ \text{Angle sensor A to C} &= cos^{-1}\left(\min\frac{X_1\times X_3+Y_1\times Y_3+Z_1\times Z_3}{\sqrt{\left({X_1}^2+{Y_1}^2+{Z_1}^2\right)\cdot\left({X_3}^2+{Y_3}^2+{Z_3}^2\right)}},1\right)\times\frac{180}{\pi}\\ \text{Angle sensor B to C} &= cos^{-1}\left(\min\frac{X_2\times X_3+Y_2\times Y_3+Z_2\times Z_3}{\sqrt{\left({X_2}^2+{Y_2}^2+{Z_2}^2\right)\cdot\left({X_3}^2+{Y_3}^2+{Z_3}^2\right)}},1\right)\times\frac{180}{\pi}\end{aligned} \quad (1)$$

where sensors X_1, Y_1, and Z_1 correspond to Sensor A; sensors X_2, Y_2, and Z_2 correspond to Sensor B; and sensors X_3, Y_3, and Z_3 correspond to Sensor C. The analysis uses the angle in degrees, by multiplying with $180/\pi$.

Standard deviation (SD): SD values are used for the population and sample between Sensors A-B, B-C, and A-C for both the right and left legs across three repeated measures (before, during, and after) on a curved path, as shown in Equation (2).

$$\sigma = \sqrt{\frac{1}{N}\left(\sum_{i=1}^{N} x_i^2 - \frac{\left(\sum_{i=1}^{N} x_i\right)^2}{N}\right)} \quad (2a)$$

$$s = \sqrt{\frac{1}{N-1}\left(\sum_{i=1}^{N} x_i^2 - \frac{\left(\sum_{i=1}^{N} {x_i}^2\right)}{N}\right)} \quad (2b)$$

In Equation (2), σ represents the standard deviation of the population, and N is the total number of data points in the population. The variable xi denotes each individual data point, while μ is the mean of these data points, calculated as shown in Equation (3). The term 's' stands for the sample standard deviation, with N representing the number of data points in the sample. Equation (2a) is used to calculate the population standard deviation (σ), and Equation (2b) is for the sample standard deviation (s). The term $\left(\sum_{i=1}^{N} {x_i}^2\right)$ represents the sum of the squares of the data points, and $\left(\sum_{i=1}^{N} x_i\right)^2$ denotes the square of the sum of the data points.

Detrended Fluctuation Analysis (DFA): Moreover, inspired by the complex fractal patterns formed through the arrangement of repetitive motifs, time series data can be analyzed using a fractal perspective. In the context of the Detrended Fluctuation Analysis (DFA) method, these fluctuations are viewed as a metric for evaluating randomness [43,44]. By quantifying the level of randomness in these fluctuations, the DFA method effectively measures the self-similarity present in the observed time series. The core principle of this method is similar to the root mean square error, but it is distinguished by its greater robustness to the non-stationary nature of the processes being analyzed [45].

Equation (3) provides the formula to compute the magnitude of fluctuations.

$$F(n) = \sqrt{\frac{1}{N}\sum_{k=1}^{N}\left[y(k) - y_n(k)\right]^2} \quad (3)$$

In Equation (3), the variable $y(k)$ represents the integral of the analyzed time series, with a total length of N, which is divided into sub-intervals of varying lengths, denoted as n. The choice of 'n' depends on the duration of the time series and the periodicity of the underlying patterns, resulting in different possible values. Simultaneously, $y_n(k)$ refers to the coefficients corresponding to the slope of the least-squares error line, typically fitted to each individual sub-interval. An investigation into the relationship between $F(n)$ and 'n' reveals a significant exponential increase in the magnitude of fluctuations as the length of the sub-intervals grows. Interestingly, this relationship appears nearly linear when viewed in a log-log scale. In particular, $F(n)$, which measures the magnitude of fluctuations, is well-approximated by n^{α}. The parameter 'α,' known as the DFA number, represents the slope of the tangent line on the log-log plot linking $F(n)$ and 'n'. This essential parameter quantifies the degree of correlation within the fluctuations [44]. The relationship between α and the stochastic nature of temporal variations throughout the successive phases is concisely represented by Equation (4).

$$\begin{cases} \propto < 0.5 & \textit{negative correlation} \\ \propto = 0.5 & \textit{zero correlation} \\ \propto > 0.5 & \textit{positive correlation} \end{cases} \quad (4)$$

The results obtained from this methodology serve a dual purpose, proving useful in the biological understanding of motor control dynamics [33]. A notable advantage of this approach is its ability to support the underlying biological framework of the central nervous system. For example, the insights gained through this method have been linked to the complex network of supra-spinal circuits involved in motor control. Additionally, these findings offer valuable perspectives on the operational mechanisms of the central pattern generator, which coordinates rhythmic motor movements [46].

4.4. Results and Discussion

4.4.1. Reliability Analysis

The ICC (Intraclass Correlation Coefficient) and Cronbach's alpha were computed to assess the reliability of the measured data. As a general guideline, values below 0.5 indicate poor reliability, those between 0.5 and 0.75 indicate moderate reliability, values from 0.75 to 0.9 indicate good reliability, and values above 0.9 indicate excellent reliability [41]. The ICC, calculated using a two-way mixed-effects model with absolute agreement, demonstrated good and high reliability, with values exceeding 0.785 for all indices (SD and DFA for both right and left legs at rest and during walking).

Additionally, Cronbach's alpha was greater than 0.793 for all indices, indicating strong internal consistency. Together, these values confirm the high reliability of the measured data (Table 1).

Table 1. Statistical reliability assessment for the measured data.

		Cronbach's Alpha (N = 12)	**ICC**	**95% Confidence Interval**	**F(44, 484)**	***p***
SD	Left rest	0.825	0.813	(0.762, 0.884)	5.703	<0.001
	Right rest	0.802	0.785	(0.754, 0.863)	5.052	<0.001
DFA	Left rest	0.857	0.857	(0.808, 0.924)	7.983	<0.001
	Right rest	0.824	0.816	(0.771, 0.877)	7.112	<0.001

Table 1. *Cont.*

		Cronbach's Alpha (N = 6)	ICC	95% Confidence Interval	F(44, 220)	p
SD	Left rest	0.890	0.844	(0.751, 0.911)	9.081	<0.001
	Right rest	0.855	0.840	(0.753, 0.903)	6.887	<0.001
DFA	Left rest	0.821	0.816	(0.762, 0.894)	5.726	<0.001
	Right rest	0.793	0.787	(0.748, 0.873)	5.104	<0.001

4.4.2. Results Evaluation

The main effect of Path, and the interactions of Path × Leg, Path × Sensor, Path × Time, Path × Time × Leg, Path × Sensor × Leg, Path × Sensor × Time, Path × Sensor × Time × Leg were not significant ($p > 0.070$) meaning that there was no significant difference between the two path even in details (Figure 7). The results, as shown in Table 2, were analyzed using ANOVA, which allowed for the comparison of different conditions and groups to determine if there were statistically significant differences in the data.

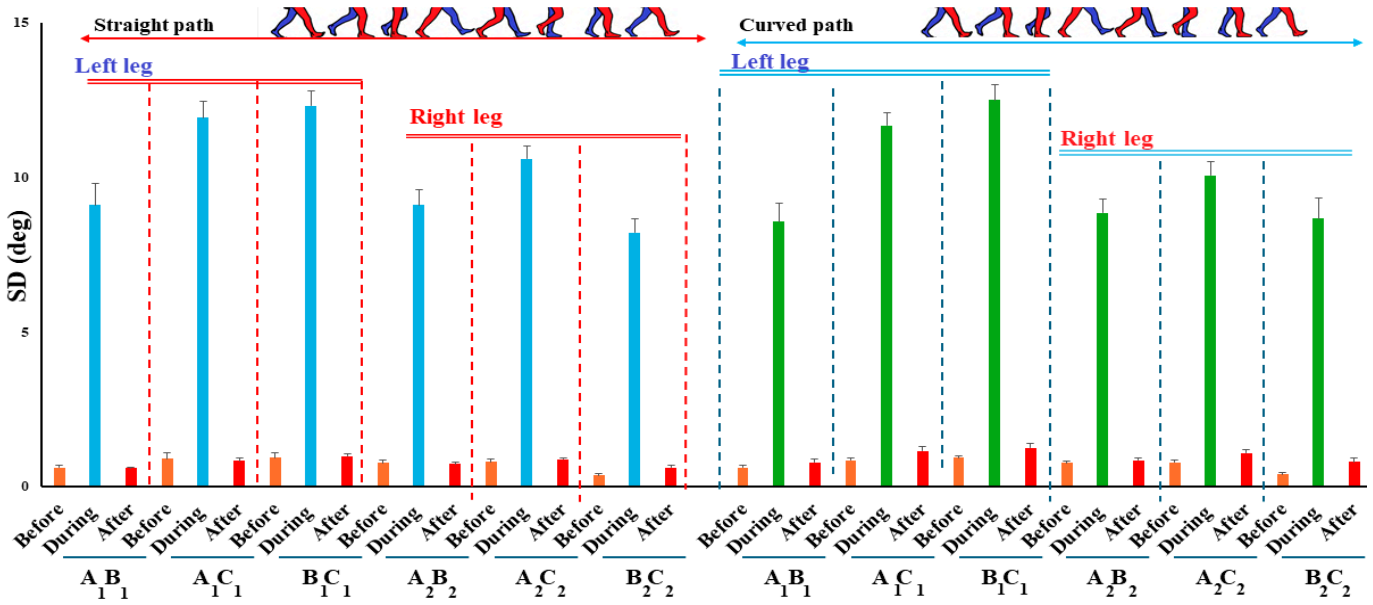


Figure 7. IoTToe design results from 45 volunteers, showing right and left leg movements for both straight and curved paths. (AB) Sensor A with respect to Sensor B; (AC) Sensor A with respect to Sensor C; (BC) Sensor B with respect to Sensor C. Results include data from standby mode before the test, during the walk on both paths, and standby mode after the walk for both legs.

As Table 2 shows, the analysis provided insights into the effectiveness of the IoTToe design and its impact on various gait parameters across different participants. The main effect of leg was significant ($F(1, 88) = 187.63$, $p = 0.003$, $\eta_P = 0.095$) because of the lower values of the right leg (3.57 ± 0.16) compared to the left leg (4.25 ± 0.16). It can be described by the majority of the participants who were right-footed. The main effect of Sensor was significant ($F(2, 176) = 40.97$, $p < 0.001$, $\eta_P = 0.318$) because of the higher values of AC combination compared to the others and lower values of the AB combination compared to the others (AB: 3.44 ± 0.13, AC: 4.29 ± 0.11, BC: 3.99 ± 0.13). The Leg × Sensor interaction was significant ($F(2, 176) = 44.04$, $p < 0.001$, $\eta_P = 0.334$). Post hoc comparisons revealed that the values for sensor combinations of AC and BC were higher in the left leg compared to the right leg (for both, $p < 0.022$). Moreover, the values of the AC were higher compared to AB and BC for both legs ($p < 0.001$). It means that the AC sensor combination is more

sensitive compared to the others. The main effect of Time was significant (F(2, 176) = 1142, $p < 0.001$, $\eta_P = 0.928$) because of the higher values of during compared to before and after (before: 0.72 ± 0.05, during: 10.13 ± 0.29, after: 0.87 ± 0.05). It means that the change between the orientations of the sensors during walking was much more than during sanding which is normal. The Leg × Time interaction was significant (F(2, 176) = 8.74, $p < 0.001$, $\eta_P = 0.090$). Posthoc comparisons revealed significant higher values in the left leg (11.02 ± 0.41) compared to the right leg (9.25 ± 0.41) just during walking ($p = 0.003$) and there was no difference between the two legs in standing positions (before and after walking, $p > 0.085$). Moreover, the values were higher during walking compared to the standing positions (i.e., before and after; for all comparisons, $p < 0.001$). The Sensor × Time interaction was significant (F(4, 352) = 28.71, $p < 0.001$, $\eta_P = 0.246$). Post hoc comparisons revealed that during walking the values of AC sensor combination were significantly higher than the others and the values of the AB sensor combination were significantly lower than the others (for all comparisons, $p < 0.015$). Moreover, for all sensor combinations, the values during walking were significantly higher than the standing positions (i.e., before and after; $p < 0.001$).

Table 2. Summary of leg- and sensor-specific variability during walking, indicating potential in-toeing and out-toeing tendencies based on AC, AB, and BC sensor combinations.

Effect/Interaction	F-Value	*p*-Value	ηP^2	Notes/Interpretation
Leg (Right vs. Left)	187.63	0.003	0.095	Left leg higher; majority right-footed participants.
Sensor (AB, AC, BC)	40.97	<0.001	0.318	AC combination highest, AB lowest; AC most sensitive.
Time (Before, During, After)	1142	<0.001	0.928	Walking phase higher than standing (before/after).
Leg × Sensor	44.04	<0.001	0.334	AC & BC higher in left leg; AC > AB, BC for both legs.
Leg × Time	8.74	<0.001	0.09	Left leg higher only during walking; walking > standing for both legs.
Sensor × Time	28.71	<0.001	0.246	AC highest, AB lowest during walking; all sensors higher during walking than standing.
Leg × Sensor × Time	21.17	<0.001	0.194	AC & BC higher in left leg; AC most sensitive for both legs during walking.
Height vs. Sensor Values	—	<0.012	—	Significant negative correlation; taller participants show less ankle variability.

It confirms the difference between the data in walking and standing positions. The Leg × Sensor × Time interaction was significant (F(4, 352) = 21.17, $p < 0.001$, $\eta_P = 0.194$). Post hoc comparisons revealed higher values in the left leg compared to right leg for AC and BC sensor combinations during walking (for both comparisons, $p < 0.012$). Furthermore, the sensitivity of the AC and BC sensor combinations was higher than AB sensor combination, while the values of AC sensor combination were higher compared to the others for both legs during walking (for all comparisons, $p < 0.002$). Pearson correlation revealed significant negative correlation between body height and the values for all sensor combinations during walking (for all, $p < 0.012$, correlation coefficients < -0.37). It confirms the effect of body height on the walking pattern. There was not a significant correlation between the values and body weight, age, and number of steps per day.

The negative correlation suggests that the taller the individual, the less variation in the ankle area for a better movement control [47]. Taller individuals generally exhibit smaller differences in angle variability. This is consistent with the idea that greater deviations in ankle alignment can cause significant deviations in the upper body, complicating the maintenance of center of pressure and balance. Moreover, the variability in the right foot was lower than the left foot, showing better control of the right foot [48]. It can be interpreted by having the majority right-footed participants. Additionally, the sensor combination of AC had a greater variability compared to the other two sensor combinations as shown in Figure 8. This implies that the number of sensors could be optimized in certain designs. For instance, sensor B, which is located on the Gastrocnemius muscle, could potentially be removed without compromising data quality.

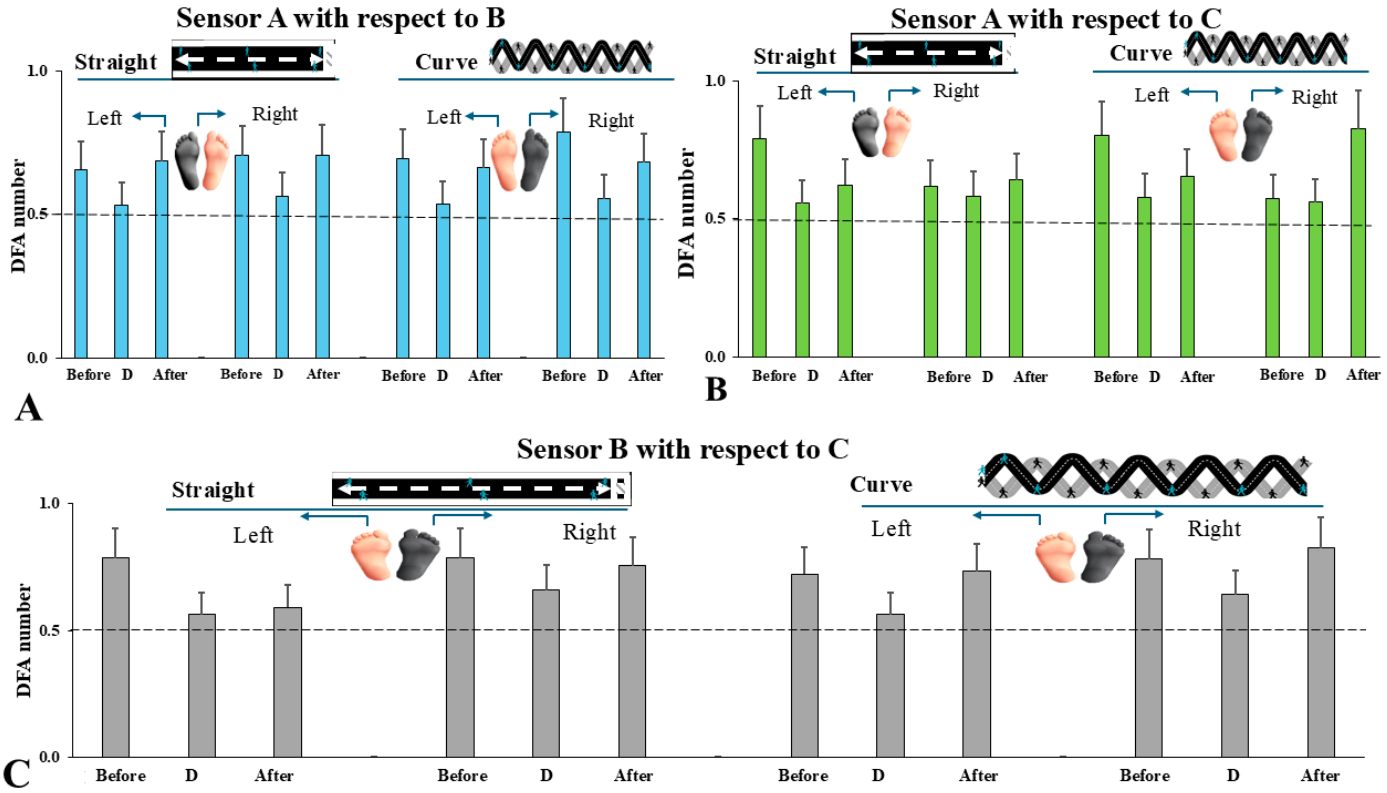


Figure 8. DFA Result Analysis: 'Before' and 'After' represent standby phases, while 'During' represents the walking phase. The line at 0.5 represents the DFA value corresponding to white noise, serving as a comparison index for analysis. The analysis displays mean values and standard errors. (**A**) Sensor A relative to Sensor B, (**B**) Sensor A relative to Sensor C, and (**C**) Sensor B relative to Sensor C.

4.5. Statistical Analysis and Results

The DFA number was analyzed using repeated measures of ANOVA with the Action (Rest, straight walking, curve walking) and Leg (right and left) as within factors.

4.5.1. The Sensor A with Respect to B

Repeated measures ANOVA on the DFA revealed a significant effect of Action ($F(2, 88) = 20.00$, $p < 0.001$, $\eta_P^2 = 0.313$), with higher values observed at rest compared to walking.

Additionally, the effect of Leg was significant ($F(1, 44) = 4.901$, $p = 0.044$, $\eta_P^2 = 0.129$), with higher values for the right leg (0.685 ± 0.016) compared to the left leg (0.564 ± 0.016). The Action $\times$ Leg interaction was not significant ($p = 0.851$).

4.5.2. Sensor A with Respect to C

Repeated measures ANOVA on the DFA revealed a significant effect of Action ($F(2, 88) = 13.24$, $p < 0.001$, $\eta_P^2 = 0.231$), with higher values observed at rest (0.679) compared to movement (0.569). However, the effect of Leg ($p = 0.298$) and the Action $\times$ Leg interaction ($p = 0.334$) were not significant.

4.5.3. Sensor B with Respect to C

Repeated measures ANOVA on the DFA revealed a significant effect of Action ($F(2, 88) = 5.72$, $p = 0.005$, $\eta_P^2 = 0.115$), with higher values at rest compared to movement. Additionally, the effect of Leg was significant ($F(1, 44) = 12.98$, $p = 0.001$, $\eta_P^2 = 0.228$), with higher values for the right leg (0.667 ± 0.018) compared to the left leg (0.594 ± 0.014). The Action $\times$ Leg interaction was not significant ($p = 0.448$).

IOTToe system is composed of six ADXL345 sensors that can be positioned in various parts of the participant's foot. The system is integrated with a webpage, empowering healthcare providers to detect and monitor the curvature process online without the need for physical tests or direct contact. The system is designed to be installed on children as young as 3 years up to adults and can be used as assistive tool during therapy or for diagnosis of in/out Toe. In balance control and walking, a DFA exponent (α) between 0.5 and 1 reflects the long-range positive correlations and suggests an adaptive, well-regulated system with a balanced degree of variability.

For Walking (Gait Variability): An α between 0.5 and 1 in walking data suggests a gait that is neither too rigid nor too random, with a balance that supports adaptability and stability. This is often seen as optimal for dynamic environments where quick, minor adjustments are needed to maintain a steady gait. This range indicates that the gait pattern has a stable structure with long-range positive correlations as we have in our results, meaning that past strides influence future strides, but not rigidly. This balance of variability suggests an adaptive gait, allowing adjustments for minor irregularities without over-correcting. Healthy young adults commonly show α values in this range, as it represents a flexible gait pattern with resilience to minor disturbances. Values closer to 1 may imply more consistent step patterns, while those closer to 0.5 reflect more variability but within a controlled range. In our results, the values for the left leg were closer to 0.5, while those for the right leg were higher, indicating more consistent control in the right leg. This can be attributed to the majority of right-footed participants in our experiment, which likely contributed to a more stable gait pattern on the dominant side.

For Balance (Postural Control in Standing): For standing balance, α between 0.5 and 1 is typically ideal, suggesting the system can effectively manage balance perturbations without excessive rigidity. Healthy individuals, especially younger adults, often show values in this range, as it allows them to respond to balance challenges with agility and minimal risk of falling. In balance control, this range suggests a stationary, adaptive postural control strategy. With α values in this range, postural sway shows correlated fluctuations, meaning small movements are adjusted through ongoing corrections, maintaining stability while allowing flexibility. This range indicates that balance adjustments are stable yet responsive to subtle shifts, which is characteristic of healthy postural control. Values closer to 0.5 show more variability and adaptability, while values closer to 1 indicate a more stable, slightly more consistent sway pattern. We should note that the higher DFA in standing balance points to a more stable, controlled posture, while the lower DFA in walking reflects the adaptability needed for dynamic movement.

The results based on ANOVA test promised to discern data of left and right leg. Moreover, we showed that the AC sensor combination was more sensitive compared to the others meaning that we can reduce the number of sensors by eliminating the sensor from

B location. Moreover, the data found a difference between left and right leg confirming the method to detect some parameters of walking. It opens a new window to realize an affordable device to detect walking parameters. Since the location of the sensors are in the lowest parts of the leg and foot, we expect this system can be used to detect some walking deformation or defect in future by recording data from healthy and patients. Taller individuals generally exhibit smaller differences in angle variability. This is consistent with the idea that greater deviations in ankle alignment can cause significant deviations in the upper body, complicating the maintenance of center of pressure and balance. Additionally, the sensor combination of AC had a greater variability compared to the other two sensor combinations. This implies that the number of sensors could be optimized in certain designs. For instance, sensor B, which is located on the Gastrocnemius muscle, could potentially be removed without compromising data quality. The results are promising for discriminating between the left and right legs. Most participants were right-footed, so better control of the right leg was expected. Our results showed that the DFA value for the left leg was lower and closer to 0.5, indicating more randomness and less long-range correlation. This suggests that the time series for the left leg behaved more like a random walk, with weak or minimal long-range correlation.

4.6. Discussion

The results of this study align with previous research highlighting the impact of foot misalignment on gait and overall health. Chronic foot malalignment, such as in-toeing or out-toeing, not only affects musculoskeletal function but can also influence mental health and quality of life due to compensatory movement strategies that may lead to secondary disorders [5]. In-toeing (pigeon toes) is often associated with structural abnormalities like metatarsus adductus or femoral anteversion, whereas out-toeing (duck feet) is commonly linked to external tibial torsion or femoral retroversion [6–8]. While many mild cases resolve naturally during growth, persistent deviations may require clinical intervention through physical therapy, orthoses, or surgery [9,10]. Idiopathic or persistent toe walking presents particular challenges, often necessitating prolonged monitoring and repeated clinical evaluations [11,12].

The present IoTToe system addresses several limitations of traditional gait assessment methods. Conventional techniques, while simple and cost-effective, often lack real-time monitoring and high sensitivity, particularly for long-term or at-home tracking [35–37]. IMU-based systems provide continuous, precise measurements of foot orientation, step length, cadence, and rotational motion, enabling detection of subtle gait deviations such as in-/out-toeing. Our results demonstrated that the AC sensor combination (instep to Achilles tendon) was most sensitive, capturing higher variability during walking, particularly in the left leg, while the right leg showed more consistent control—likely reflecting the dominance of right-footed participants. This finding is consistent with previous literature suggesting dominant-leg stability reduces angular variability in gait [48].

Statistical analyses, including repeated-measures ANOVA and DFA, confirmed the system's ability to detect significant differences between legs and sensor combinations, as well as gait versus standing conditions. For instance, DFA values during walking were lower for the left leg (closer to 0.5), suggesting greater variability and adaptive gait behavior, whereas the right leg showed higher DFA values, indicating more stable and controlled steps. The AC sensor combination demonstrated the highest sensitivity, implying that sensor placement could be optimized by potentially eliminating less informative sensors, such as sensor B on the gastrocnemius. Furthermore, taller participants exhibited smaller angle variability, consistent with prior findings that ankle alignment deviations influence upper-body stability and center-of-pressure maintenance.

Following established approaches for wearable data quality assessment [49,50], we evaluated the quality of the recorded signals using intraclass correlation coefficients (ICC) and detrended fluctuation analysis (DFA) to assess signal consistency and temporal structure, thereby ensuring the reliability of the wearable monitoring data. Additionally, our multi-MCU, multi-sensor platform follows the smart wearable standards for health monitoring discussed by Andreu-Perez et al. (2015) [51] and Deng et al. (2023) [52].

Furthermore, we would like to add that the IoTToe system utilizes a total of three NodeMCU microcontrollers and six ADXL345 sensors distributed across both legs. As shown in the system design, each of the three discrete wearable units consists of two ADXL345 sensors connected to one NodeMCU. This 2:1 sensor-to-MCU ratio allows for tight hardware-level synchronization via a wired I2C bus, ensuring that the paired sensors on each unit are sampled simultaneously by a single master clock. Moreover, statistical reliability while the data recording can be sensitive to jitter, the system's empirical reliability is confirmed by high-resolution metrics:

- Internal Consistency: Cronbach's alpha values exceeded 0.793, indicating high internal consistency across all indices.
- Reliability: Intraclass Correlation Coefficient (ICC) values reached up to 0.911, demonstrating "good to high" reliability in capturing gait dynamics.
- Stability: DFA was used to quantify signal randomness. Values remained between 0.5 and 1.0, confirming persistent long-range correlations and that the captured data reflects stable patterns rather than white noise from sampling jitter.

Moreover, to handle the data flow from multiple MCUs, the system employs a real-time transfer protocol to a central web monitoring page. Data is subsequently downloaded into a single Excel file, allowing for synchronized temporal alignment during secondary analysis. Our results successfully distinguished significant, consistent differences in Leg $\times$ Sensor interactions (e.g., right leg values of 3.57 ± 0.16 vs. left leg at 4.25 ± 0.16), proving that network "dilation" did not impair the detection of biomechanical variations.

Based on the results, potential in-toeing or out-toeing can be inferred from leg-specific patterns and sensor combinations:

- **Leg differences:**
  - ✓ The left leg exhibited higher variability than the right leg during walking.
  - ✓ The right leg showed lower variability, consistent with most participants being right-footed.
  - ✓ Greater variability often reflects increased deviations in ankle orientation, potentially indicating mild in- or out-toeing.
- **Sensor combinations:**
  - ✓ The AC sensor combination (instep to Achilles tendon) showed the highest variability in both legs, suggesting more medial-lateral or rotational foot motion.
  - ✓ The AB combination (instep to gastrocnemius) had the lowest variability, indicating minimal rotational deviation.
- **Walking vs. standing:**
  - ✓ Differences were prominent during walking, not standing, indicating that in-/out-toeing manifests primarily during dynamic gait.
- **Interpretation:**
  - ✓ Participants with higher AC sensor values in the left leg during walking may exhibit more in- or out-toeing on that side.
  - ✓ The right leg is generally more stable, showing less toe deviation.

✓ While AC sensor values are most indicative of rotational foot motion, exact in-/out-toeing direction requires confirmation via angle orientation measurements.

5. Conclusions

Toe-in and toe-out foot alignment refers to the inward or outward angle of the toes, which can affect gait, posture, and joint stress. Detecting and monitoring these alignments, along with assessing improvements, are crucial for managing their impact on individuals. Exact global numbers are not available, many individuals experience internal or external foot rotation unknowingly, particularly during activities like walking, running, or sitting. Chronic pronation, where the foot turns inward during walking, can lead to various health issues. Prolonged pronation may cause an abnormal gait, increasing pressure on the knee, hip, and spine, resulting in pain and fatigue in these areas. It can also contribute to arch collapse, heightened plantar pressure, and conditions like flat feet and plantar fasciitis. Additionally, long-term pronation affects ankle stability, elevating the risk of sprains and injuries. Conversely, sustained external foot rotation may lead to excessively raised arches, elevated plantar pressure, and conditions such as high arches and plantar warts. It can also destabilize the inner ankle, increasing the likelihood of sprains. Abnormal gait patterns from prolonged external rotation can further strain the knee, hip, and spine, causing discomfort and fatigue. In this paper, we propose a wearable IOT device called IoTToe and investigate its performance with 45 participants (36 men and 9 women) aged 20 to 25 years, each with varying BMI indices. The average age for males is 21.58 years and for females is 21.45 years. Sample sizes were calculated using G-Power software.

Limitations of this study include a relatively small, convenience-based sample restricted to healthy young adults, which may limit generalizability. The system was not yet tested on clinical populations or children with severe gait abnormalities, which may present distinct movement patterns. Additionally, while IMU sensors provide precise rotational data, calibration and placement errors may introduce variability, and the system does not yet measure exact joint angles for direct classification of in- versus out-toeing.

Despite these limitations, the IoTToe design demonstrates significant promise for affordable, long-term gait monitoring. It offers clinicians and caregivers real-time, multi-point foot motion data, with potential applications for early detection of gait deviations, treatment monitoring, and rehabilitation guidance. Future studies should focus on validating the system in clinical populations, refining sensor placement, and integrating angle-specific measurements to improve classification of in-/out-toeing patterns.

In summary, the proposed design boasts advantages across multiple dimensions, including comprehensive data collection, accuracy, and reliability, enhanced user experience and portability, and significant potential for clinical applications. These strengths not only make the project highly valuable but also pave the way for significant advancements and innovations in the realms of gait monitoring and rehabilitation therapy. IOTToe design represents not only a technological innovation but also a compassionate approach to human health. It has the potential to reshape how foot health is understood and managed, offering a healthier and more comfortable life. The system's successful outcomes underscore its potential for telemetric applications in hospital environments, providing valuable insights and data for medical professionals and researchers. It can monitor and analyze critical parameters remotely, thereby enhancing healthcare efficiency and supporting advanced research in various medical fields. Future work will focus on optimizing the hardware design, such as integrating all six sensors via a single NodeMCU to reduce complexity and power consumption. Data collection will be expanded to include clinical populations, children with gait abnormalities, and individuals with confirmed toe-in or toe-out alignment. Additionally, the web-based interface will be enhanced to provide clinically meaningful

outputs, including automated toe-in/toe-out detection, gait classification, and decision-support functionalities. Increasing the sample size, particularly for female participants, will improve generalizability and provide more comprehensive insights into gait patterns and related complications.

Author Contributions: Conceptualization, A.J.M. and Z.K.; methodology, A.J.M.; software, Z.W.; validation, Z.W., Z.K. and M.E.A.; formal analysis, A.J.M.; investigation, Z.K. and A.J.M.; resources, M.E.A.; data curation, A.J.M.; writing—original draft preparation, A.J.M.; writing—review and editing, Z.K. and A.J.M.; visualization, Z.W.; supervision, A.J.M.; project administration, M.E.A. All authors have read and agreed to the published version of the manuscript.

Funding: This research received no external funding.

Institutional Review Board Statement: The study was conducted in accordance with the ethical standards set forth by the Declaration of Helsinki, and the approval was obtained by the Institutional Review Board (IRB) at RARL, Jiangxi University of Science and Technology (protocol code: 2024JXUST730 and date of approval: 30 July 2024).

Informed Consent Statement: Informed consent was obtained from all subjects involved in the study.

Data Availability Statement: All the data used in the research can be obtained from the corresponding author on suitable request.

Acknowledgments: The authors would like to thank RARL (Robotic Automation Research Lab), School of Information Engineering, Jiangxi University of Science and Technology, Ganzhou 341000, China. The designed system has been officially registered with the National Copyright Administration of the People's Republic of China as both hardware and software under the name Foot Alignment Check System 1.0 (Software Registration Number: 2024R11L0825282) on 6 June 2024.

Conflicts of Interest: The authors declare no conflicts of interest.

Abbreviations

The following abbreviations are used in this manuscript:

ANOVA	Analysis of Variance
AJAX	Asynchronous JavaScript and XML
BMI	Body Mass Index
CoP	Center of Pressure
CP	Cerebral Palsy
DAFO	Dual Adaptive Frequency Oscillator
DFA	Discriminant Function Analysis
ICC	Intra-Class Correlation Coefficient
IMU	Inertial Measurement Unit
IoT	Internet of Things
LSTM	Long Short-Term Memory
PPD	Plantar Pressure Distribution
SD	Standard Deviation

Appendix A

Appendix A.1. The Review Summary

Ref	Target/Application	Sensors and Data	Method/Algorithm	Key Results/Main Contribution
[14]	Toe-walking severity in children with CP	Sensorized shoe (CoP, ankle kinematics)	Feature extraction + classifier	High accuracy in predicting toe-walking severity Demonstrated feasibility of objective, frequent gait assessment

Ref	Target/Application	Sensors and Data	Method/Algorithm	Key Results/Main Contribution
[15]	Gait phase detection	FSRs + IMUs	Fuzzy logic	Improved detection vs. existing methods; errors mainly in stance phase Intelligent gait-phase detection with real-time feedback
[16]	Assistive mobility for toddlers	Foot-motion control + camera	Bio-driven control interface	All subjects navigated maze successfully Intuitive foot-controlled assistive device for motor development
[17]	Gait deviation severity (CP)	Sensorized shoe (CoP)	Random Forest	>80% field accuracy; >90% home-based accuracy Longitudinal, home-based gait monitoring system
[18]	Pathological gait detection	Insole pressure + EMG	Cross-correlation gait map	Clear distinction between normal and pathological gait Multi-modal wearable gait biomechanics assessment
[19]	Real-time gait phase estimation	IMUs	LSTM + DAFO	98.58% accuracy; toe-off error ≈15 ms, Robust multi-locomotion gait phase estimation
[20]	Foot Progression Angle (FPA) modification	IMU + magnetometer + haptics	Feedback control	MAE ≈ 3.1°; improved with reduced no-feedback window, Portable FPA correction via haptic feedback
[21]	Ankle angle and toe clearance	Ultrasonic sensors	Geometric triangulation	r = 0.98 (AA), r = 0.99 (MTC) IMU-drift-free continuous gait monitoring
[22]	Real-time gait monitoring	In-shoe sensors	Optimized sampling + PCA	<2.1% error in key gait parameters High-fidelity, bandwidth-optimized gait system
[23]	Plantar pressure distribution	Self-calibrating in-shoe sensors	Adaptive FMR calibration	CV reduced via in-shoe characterization Highlighted importance of sensor calibration
[24]	FPA estimation	Single IMU	Dynamic step-frame estimation	Mean error $\leq 2.6°$ Magnetometer-free FPA estimation
[25]	Pediatric gait classification	8 × 8 pressure array	ML-based IGRM	Up to 97.79% intra-subject accuracyReal-time pathological gait recognition
[26]	FPA measurement	Force plate	CoP-based method	MAE ≈ 2.0–3.3° Accurate FPA estimation without kinematics

Ref	Target/Application	Sensors and Data	Method/Algorithm	Key Results/Main Contribution
[27]	Toe-walking rehabilitation	Smart insole (pressure + vibration)	Rule-based detection	91.3% classification accuracy Remote monitoring and feedback for toe walking
[28]	Gait analysis review	IMUs and insoles	Rule-based methods	Identified HS/TO as key events Comprehensive survey of wearable gait systems
[29]	FPA detection	Plantar pressure images	YOLOv4	AP $\approx$ 100%; error $\approx 0.1^{\circ}$ Deep-learning-based FPA estimation
[30]	Gait event detection (CP)	Foot markers	LSTM	IC: 89.7%; TO: 71.6% Automated gait-event detection in CP
[31]	Gait abnormality correction	Pressure + IMU	IoT-based monitoring	56.25% (toe-in), 81.25% (toe-out) Real-time IoT gait correction platform

Appendix A.2. Self-Declaration Form

According to the provisions of the test, I hereby express my consent to participate in this research and allow presenting the obtained results in the journals and scientific circles without mentioning my name and I will not have any complaints in this regard in the future. Participant Name/date/signature.

Appendix A.3. Participant Data

	(A) Demographic Information:
1	Height (in cm)
2	Weight (in kilograms)
3	Age (in years)
4	Gender (Male/Female/Other)
5	Level of Education (in years, calculated from the first class of elementary school)
6	Footedness: Are you left-footed or right-footed? (kicking a ball)
	(B) Medical and Health Information:
1	Do you have any underlying diseases? If yes, please specify.
2	Do you wear glasses? What are the diopter values for the left and right eyes?
3	Walking Pain: Do you experience any pain while walking? (Yes/No)
4	Walking Experience: Have you experienced any falls while walking? (Yes/No)
5	Do you use handrails or support when walking on stairs or inclines? (Yes/No)
6	How would you rate your overall walking ability? (Excellent/Good/Fair/Poor)

	(C) Usage and Habits:
1	Camera and Binoculars Usage: Do you frequently use cameras or binoculars? If yes, please specify the duration of usage (hours per day or week)
2	Shoe Soles Usage: How long do you use shoe soles before replacing them? (More than a month/Less than a month)
3	Insole Status: Are your insoles newly purchased? (Yes/No)
4	Walking Habits: How many steps do you typically walk in a day?
5	Do you walk on uneven terrain regularly? (Yes/No)
6	Do you use walking aids such as canes or walkers? (Yes/No)
7	Do you engage in regular physical exercise? (Yes/No)
8	Do you walk for transportation or recreation? (Transportation/Recreation/Both)
	(D) Footwear Preferences and Conditions:
1	Footwear: Do you wear orthopedic shoes? (Yes/No)
2	Are your shoes comfortable for walking long distances? (Yes/No)
3	Do you prefer specific shoe brands or types for walking? (Specify)
	(E) Walking Environment:
1	Do you walk indoors, outdoors, or both? (Yes/No)
2	Do you encounter obstacles or hazards while walking? (Yes/No)
3	How often do you walk on stairs or inclines?

Notice: This form should be signed by each participant before test.

References

1. Marta, G.; Quental, C.; Folgado, J.; Guerra-Pinto, F. Multibody modelling of the foot for the biomechanical analysis of the ankle joint during running: A narrative review. *Proc. Inst. Mech. Eng. Part K J. Multi-Body Dyn.* **2022**, *236*, 338–353. [CrossRef]
2. Aguillard, E.; Cane, J.; Goldstein, A.L. *Run Healthy: The Runner's Guide to Injury Prevention and Treatment*; Human Kinetics: Champaign, IL, USA, 2023.
3. Raj, N.B.; Lee, W.Z.; Eswaramoorthi, V.; Razali, H.; Othman, N.Y.H.; Rao, U. Exercise programmes for reducing the risk of falls in elderly: A review. *Res. J. Pharm. Technol.* **2020**, *13*, 2977–2984. [CrossRef]
4. Yanardag, M.; Şimşek, T.T.; Yanardag, F. Exploring the relationship of pain, balance, gait function, and quality of life in older adults with hip and knee pain. *Pain Manag. Nurs.* **2021**, *22*, 503–508. [CrossRef]
5. Razmjou, H.; Savona, A.; Szafirowicz, A.; Deel, L.; Richards, R. Psychosocial risk factors and physical and mental well-being following a compensable knee injury. *Eur. J. Physiother.* **2023**, *25*, 100–105. [CrossRef]
6. Pathak, P.; Kim, H.S.; Kim, H.; Park, J.; Lee, G.; Ahn, J. Feasibility of mitigating out-toeing gait using compression tights with inward-directing taping lines. *PLoS ONE* **2023**, *18*, e0291914. [CrossRef]
7. Bent, M.A.; Stork, N.C.; Nemeth, B.A. The diagnosis and management of common childhood orthopedic disorders: An update. *Curr. Probl. Pediatr. Adolesc. Health Care* **2020**, *50*, 100884. [CrossRef]
8. Honig, E.L.; Haeberle, H.S.; Kehoe, C.M.; Dodwell, E.R. Pediatric orthopedic mythbusters: The truth about flexible flatfeet, tibial and femoral torsion, w-sitting, and idiopathic toe-walking. *Curr. Opin. Pediatr.* **2021**, *33*, 105–113. [CrossRef]
9. Jin, S.; Xu, C.; Cai, H.; Chen, C.; Lu, Y.; Wang, Z.; Shen, M. Comparative analysis of physical examination, CT scan, and three-dimensional gait analysis in evaluating lower extremity torsion deformities in children with cerebral palsy. *Med. Sci. Monit.* **2023**, *29*, e940948. [CrossRef] [PubMed]
10. Cao, L.A.; Rethlefsen, S.A.; Wren, T.A.; Kay, R.M. Causes of out-toeing gait in children with cerebral palsy. *Gait Posture* **2020**, *76*, 141–145. [CrossRef]
11. Sala, D.A. Idiopathic toe-walking: A review from 1967 to 2021. *J. Pediatr. Neurol.* **2022**, *20*, 237–251. [CrossRef]
12. Cao, L.A.; Wimberly, L. When to be concerned about abnormal gait: Toe walking, in-toeing, out-toeing, bowlegs, and knock-knees. *Pediatr. Ann.* **2022**, *51*, E340–E345. [CrossRef]

13. Moshayedi, A.J.; Iskar, I.; Yang, S.; Shinde, S.K.; Razi, A.; Andani, M.E. IOTToe: A Smart System for In/Out-Toeing Foot Identification. In Proceedings of the 2024 6th International Conference on Communications, Information System and Computer Engineering (CISCE), Guangzhou, China, 10–12 May 2024; IEEE: Piscataway, NJ, USA, 2024.
14. Mancinelli, C.; Patel, S.; Deming, L.C.; Schmid, M.; Patritti, B.L.; Chu, J.J.; Beckwith, J.; Greenwald, R.; Healey, J.; Bonato, P. Assessing the feasibility of classifying toe-walking severity in children with cerebral palsy using a sensorized shoe. In Proceedings of the 2009 Annual International Conference of the IEEE Engineering in Medicine and Biology Society, Minneapolis, MN, USA, 3–6 September 2009; IEEE: Piscataway, NJ, USA, 2009; pp. 5163–5166.
15. Senanayake, C.M.; Senanayake, S.A. Computational intelligent gait-phase detection system to identify pathological gait. *IEEE Trans. Inf. Technol. Biomed.* **2010**, *14*, 1173–1179. [CrossRef]
16. Schoepflin, Z.R.; Chen, X.; Ragonesi, C.B.; Galloway, J.C.; Agrawal, S.K. Design of a novel mobility device controlled by the feet motion of a standing child: A feasibility study. *Med. Biol. Eng. Comput.* **2011**, *49*, 1225–1231. [CrossRef]
17. Mancinelli, C.; Patel, S.; Deming, L.C.; Nimec, D.; Chu, J.J.; Beckwith, J.; Greenwald, R.; Bonato, P. A novel sensorized shoe system to classify gait severity in children with cerebral palsy. In Proceedings of the 2012 Annual International Conference of the IEEE Engineering in Medicine and Biology Society, San Diego, CA, USA, 28 August–1 September 2012; IEEE: Piscataway, NJ, USA, 2012; pp. 5010–5013.
18. Faragó, P.; Grama, L.; Farago, M.-A.; Hintea, S. A novel wearable foot and ankle monitoring system for the assessment of gait biomechanics. *Appl. Sci.* **2020**, *11*, 268. [CrossRef]
19. Zhang, X.; Zhang, H.; Hu, J.; Zheng, J.; Wang, X.; Deng, J.; Wan, Z.; Wang, H.; Wang, Y. Gait pattern identification and phase estimation in continuous multilocomotion mode based on inertial measurement units. *IEEE Sens. J.* **2022**, *22*, 16952–16962. [CrossRef]
20. Xia, H.; Charlton, J.M.; Shull, P.B.; Hunt, M.A. Portable, automated foot progression angle gait modification via a proof-of-concept haptic feedback-sensorized shoe. *J. Biomech.* **2020**, *107*, 109789. [CrossRef]
21. Mani, N.; Haridoss, P.; George, B. A wearable ultrasonic-based ankle angle and toe clearance sensing system for gait analysis. *IEEE Sens. J.* **2020**, *21*, 8593–8603. [CrossRef]
22. Wu, J.; Kuruvithadam, K.; Schaer, A.; Stoneham, R.; Chatzipirpiridis, G.; Easthope, C.A.; Barry, G.; Martin, J.; Pané, S.; Nelson, B.J.; et al. An intelligent in-shoe system for gait monitoring and analysis with optimized sampling and real-time visualization capabilities. *Sensors* **2021**, *21*, 2869. [CrossRef]
23. Martínez-Barba, D.A.; Martínez-Manuel, R.; Daza-Benítez, L.; Vidal-Lesso, A. Development of self-calibrating sensor footwear and relevance of in-shoe characterization on accurate plantar pressure distribution measurements. *IEEE Sens. J.* **2020**, *21*, 8421–8431. [CrossRef]
24. Wouda, F.J.; Jaspar, S.L.; Harlaar, J.; van Beijnum, B.-J.F.; Veltink, P.H. Foot progression angle estimation using a single foot-worn inertial sensor. *J. Neuroeng. Rehabil.* **2021**, *18*, 37. [CrossRef] [PubMed]
25. Xu, L.; Chen, J.; Wang, F.; Chen, Y.; Yang, W.; Yang, C. Machine-learning-based children's pathological gait classification with low-cost gait-recognition system. *Biomed. Eng. Online* **2021**, *20*, 62. [CrossRef]
26. Caderby, T.; Begue, J.; Dalleau, G.; Peyrot, N. Measuring foot progression angle during walking using force-plate data. *Appl. Mech.* **2022**, *3*, 174–181. [CrossRef]
27. Ershadi, G.; Gwak, M.; Aminian, A.; Soangra, R.; Grant-Beuttler, M.; Sarrafzadeh, M. Smart insole: Remote gait detection algorithm using pressure sensors for toe walking rehabilitation. In Proceedings of the 2021 IEEE 7th World Forum on Internet of Things (WF-IoT), New Orleans, LA, USA, 14 June–31 July 2021; IEEE: Piscataway, NJ, USA, 2021; pp. 332–337.
28. Prasanth, H.; Caban, M.; Keller, U.; Courtine, G.; Ijspeert, A.; Vallery, H.; Von Zitzewitz, J. Wearable sensor-based real-time gait detection: A systematic review. *Sensors* **2021**, *21*, 2727. [CrossRef]
29. Ardhianto, P.; Subiakto, R.B.R.; Lin, C.-Y.; Jan, Y.-K.; Liau, B.-Y.; Tsai, J.-Y.; Akbari, V.B.H.; Lung, C.-W. A deep learning method for foot progression angle detection in plantar pressure images. *Sensors* **2022**, *22*, 2786. [CrossRef]
30. Kim, Y.K.; Visscher, R.M.; Viehweger, E.; Singh, N.B.; Taylor, W.R.; Vogl, F. A deep-learning approach for automatically detecting gait-events based on foot-marker kinematics in children with cerebral palsy—Which markers work best for which gait patterns? *PLoS ONE* **2022**, *17*, e0275878. [CrossRef] [PubMed]
31. Lee, S.Y. IoT-Based Sensor Shoes System for Gait Correction. *Int. J. Electr. Electron. Res.* **2022**, *10*, 62–68. [CrossRef]
32. Cao, Y.; Zhuang, H.; Zhang, X.; Guo, R.; Pang, H.; Zheng, P.; Xu, H. Impact of foot progression angle on spatiotemporal and plantar loading pattern in intoeing children during gait. *Sci. Rep.* **2024**, *14*, 14402. [CrossRef]
33. Singh, J.P.; Jain, S.; Arora, S.; Singh, U.P. Vision-based gait recognition: A survey. *IEEE Access* **2018**, *6*, 70497–70527. [CrossRef]
34. Zago, M.; Luzzago, M.; Marangoni, T.; De Cecco, M.; Tarabini, M.; Galli, M. 3D tracking of human motion using visual skeletonization and stereoscopic vision. *Front. Bioeng. Biotechnol.* **2020**, *8*, 181. [CrossRef] [PubMed]
35. Rani, V.; Kumar, M. Human gait recognition: A systematic review. *Multimed. Tools Appl.* **2023**, *82*, 37003–37037. [CrossRef]
36. Bauer, L.; Hamberger, M.A.; Böcker, W.; Polzer, H.; Baumbach, S.F. Development of an imu based 2-segment foot model for an applicable medical gait analysis. *BMC Musculoskelet. Disord.* **2024**, *25*, 606. [CrossRef]

37. Donne, J.H.; Powell, J.A.; Fahey, M.C.; Beare, R.; Kolic, J.; Williams, C.M. Some children with idiopathic toe walking display sensory processing difficulties but not all: A systematic review. *Acta Paediatr.* **2023**, *112*, 1620–1632. [CrossRef]
38. Hodges, A.C.; Wilder, D.A.; Ertel, H. Assessment and treatment of toe walking. In *Handbook of Applied Behavior Analysis: Integrating Research into Practice*; Springer: Berlin/Heidelberg, Germany, 2023; pp. 1199–1214.
39. Faul, F.; Erdfelder, E.; Lang, A.-G.; Buchner, A. G* power 3: A flexible statistical power analysis program for the social, behavioral, and biomedical sciences. *Behav. Res. Methods* **2007**, *39*, 175–191. [CrossRef] [PubMed]
40. Yawar, A.; Lieberman, D.E. Biomechanical tradeoffs in foot function from variations in shoe design. *Exerc. Sport Sci. Rev.* **2023**, *51*, 128–139. [CrossRef]
41. Koo, T.K.; Li, M.Y. A guideline of selecting and reporting intraclass correlation coefficients for reliability research. *J. Chiropr. Med.* **2016**, *15*, 155–163. Erratum in *J. Chiropr. Med.* **2017**, *16*, 346. [CrossRef]
42. Cohen, J. *Statistical Power Analysis for the Behavioral Sciences*; Routledge: Oxfordshire, UK, 2013.
43. Hausdorff, J.M.; Peng, C.-K.; Ladin, Z.; Wei, J.Y.; Goldberger, A.L. Is walking a random walk? evidence for long-range correlations in stride interval of human gait. *J. Appl. Physiol.* **1995**, *78*, 349–358. [CrossRef] [PubMed]
44. Peng, C.-K.; Mietus, J.; Hausdorff, J.; Havlin, S.; Stanley, H.E.; Goldberger, A.L. Long-range anticorrelations and non-Gaussian behavior of the heartbeat. *Phys. Rev. Lett.* **1993**, *70*, 1343–1346. [CrossRef]
45. Terrier, P.; Dériaz, O. Kinematic variability, fractal dynamics and local dynamic stability of treadmill walking. *J. Neuroeng. Rehabil.* **2011**, *8*, 12. [CrossRef] [PubMed]
46. Hausdorff, J.; Schaafsma, J.; Balash, Y.; Bartels, A.; Gurevich, T.; Giladi, N. Impaired regulation of stride variability in parkinson's disease subjects with freezing of gait. *Exp. Brain Res.* **2003**, *149*, 187–194. [CrossRef]
47. Mumtaz, N.; Arif, S.; Qadeer, N.; Khan, Z.H. Development of a low cost wireless IMU using MEMS sensors for pedestrian navigation. In Proceedings of the 2017 International Conference on Communication, Computing and Digital Systems (C-CODE), Islamabad, Pakistan, 8–9 March 2017; pp. 310–315. [CrossRef]
48. Khan, Z.; Arif, M.; Kattan, A.; Ali, S.; Munawar, K. Pedestrian tracking using MEMS based wireless inertial measurement unit. In Proceedings of the 4th International Conference on Computer Engineering Mathematical Sciences (ICCEMS 2015), Lankawi, Malaysia, 10–11 December 2015.
49. Böttcher, S.; Vieluf, S.; Bruno, E.; Joseph, B.; Epitashvili, N.; Biondi, A.; Zabler, N.; Glasstetter, M.; Dümpelmann, M.; Van Laerhoven, K.; et al. Data quality evaluation in wearable monitoring. *Sci. Rep.* **2022**, *12*, 21412. [CrossRef]
50. Zschocke, J.; Leube, J.; Glos, M.; Semyachkina-Glushkovskaya, O.; Penzel, T.; Bartsch, R.; Kantelhardt, J. Reconstruction of Pulse Wave and Respiration From Wrist Accelerometer During Sleep. *IEEE Trans. Biomed. Eng.* **2022**, *69*, 830–839. [CrossRef] [PubMed]
51. Andreu-Perez, J.; Leff, D.R.; Ip, H.M.D.; Yang, G.Z. From Wearable Sensors to Smart Implants-Toward Pervasive and Personalized Healthcare. *IEEE Trans. Biomed. Eng.* **2015**, *62*, 2750–2762. [CrossRef] [PubMed]
52. Deng, Z.; Guo, L.; Chen, X.; Wu, W. Smart Wearable Systems for Health Monitoring. *Sensors* **2023**, *23*, 2479. [CrossRef] [PubMed]

Disclaimer/Publisher's Note: The statements, opinions and data contained in all publications are solely those of the individual author(s) and contributor(s) and not of MDPI and/or the editor(s). MDPI and/or the editor(s) disclaim responsibility for any injury to people or property resulting from any ideas, methods, instructions or products referred to in the content.